

Non-adiabatic effects in the irradiation of ethylene

Z.P. Wang,^{1,2,3,4,5} P.M. Dinh,^{4,5*} P.-G. Reinhard,⁶ E. Suraud,^{4,5} and F.S. Zhang^{2,3}

¹*School of Science, JiangNan University, Wuxi 214122, China*

²*The Key Laboratory of Beam Technology and Material Modification of Ministry of Education, College of Nuclear Science and Technology, Beijing Normal University, Beijing 100875, People's Republic of China*

³*Beijing Radiation Center, Beijing 100875, China*

⁴*Université de Toulouse; UPS; Laboratoire Physique Théorique (IRSAMC), F-31062 Toulouse, France*

⁵*CNRS; LPT(IRSAMC), F-31062 Toulouse, France*

⁶*Institut für Theoretische Physik, Universität Erlangen, Staudtstrasse 7, D-91058 Erlangen, Germany*

In the framework of the time dependent local density approximation, applied to valence electrons, coupled non-adiabatically to molecular dynamics of ions, the irradiations of ethylene by laser and fast charged projectiles are studied. We find that the Coulomb fragmentation sensitively depends on the laser frequency and on the charge of the projectile.

1. Introduction

It is well known that the interaction of ionizing radiation with biological tissue can induce severe damage to DNA.^{1,2} With the development of ion sources such as the electron cyclotron resonance (ECR) ion source and modern accelerators such as cooling storage ring (CSR), a lot of investigations have been devoted to understanding the molecular mechanisms underlying biological radiation damage. More recently, a number of experimental investigations have been addressed concerning the action of ions on molecules with high and low energies.^{3–12} From the mass spectra, the relative cross sections for the different ionization and fragmentation channels can be evaluated. One can observe not only the process of electron capture but also the highly excited processes, such as electronic emission and Coulomb explosion due to the induced ionization.

Impact of radiation also includes excitation by photons and we will discuss their effects as well. The advantage of photons is that modern lasers provide flexible and powerful pulses for studies of photo-induced dynamics, such as optical response,¹³ multi-photon ionization,¹⁴ and Coulomb explosion of clusters,¹⁵ high-order harmonic generation,^{16–18} bond softening,^{19,20} and charge resonance enhanced ionization.^{21,22}

*Corresponding author. Email: dinh@irsamc.ups-tlse.fr

The perfect theoretical description of these mechanisms would require to solve the time-dependent Schrödinger equation for all electrons and all nuclear degrees of freedom. However, this ultimate attack exists only for very small systems, such as atoms,^{23,24} H_2 and H_2^+ .^{25–29} For larger systems, more approximate ways have to be found. Recently, Horsfield *et al.* used correlated electron-ion dynamics to study the excitation of atomic motion by energetic electrons.³⁰ Saalman *et al.* have developed a non-adiabatic quantum molecular dynamics (NA-QMD) to study different non-adiabatic processes in different systems^{31–33} and Calvo *et al.* used a combined method to study the fragmentation of rare-gas clusters.³⁴ It is also interesting to develop a fully-fledged coupled ionic and electronic dynamics. At the side of electronic dynamics, the well tested Time-Dependent Density Functional Theory at the level of the Time-Dependent Local Density Approximation (TDLDA)³⁵ is used. The ions are treated by classical molecular dynamics (MD). This altogether provides a coupled TDLDA-MD, for a review see.³⁶ Up to now, this approach has been applied to study the dynamical scenarios of simple metal and hydrogen clusters.^{37–43} Besides these systems, organic molecules are particularly interesting cases and recently motivated a lot of theoretical works to investigate either the optical response in the linear domain⁴⁴ or the dynamics of it without and with considering the external laser field.^{33,45}

In this paper, the irradiations of ethylene by laser and fast charged projectiles are studied by using a coupled TDLDA-MD³⁶ and various non-adiabatic effects are investigated. The paper is organized as follows. Section 2 provides a short presentation of the theoretical and numerical approach. Section 3 first gives the optical response properties of ethylene and the effect of ionic motion on the excitation dynamics is discussed. Then different excitation scenarios of ethylene as a function of the laser frequency and charged projectiles are presented. Section 4 gives some conclusions.

2. Theory

In this section, we briefly represent the real-time method in TDLDA-MD. The molecule is described as a system composed of valence electrons and ions. Our test case, the ethylene molecule C_2H_4 , has 12 valence electrons and 6 ions. The interaction between ions and electrons is described by means of norm-conserving pseudopotentials.⁴⁶

Valence electrons are treated by TDLDA, augmented with an average-density self-interaction correction (ADSIC).⁴⁷ They are represented by single-particle orbitals $\phi_j(\mathbf{r}, t)$ satisfying the time-dependent Kohn-Sham (TDKS) equations,⁴⁸

$$i\frac{\partial}{\partial t}\phi_j(\mathbf{r}, t) = \hat{H}_{\text{KS}}\phi_j(\mathbf{r}, t) = \left(-\frac{\nabla^2}{2m_{\text{el}}} + V_{\text{eff}}(\mathbf{r}, t)\right)\phi_j(\mathbf{r}, t), \quad j = 1, \dots, N. \quad (1)$$

The term V_{eff} stands for the Kohn-Sham effective potential and is composed of four parts,

$$V_{\text{eff}}(\mathbf{r}, t) = V_{\text{ion}}(\mathbf{r}, t) + V_{\text{ext}}(\mathbf{r}, t) + V_{\text{H}}[n](\mathbf{r}, t) + V_{\text{xc}}[n](\mathbf{r}, t), \quad (2)$$

where $V_{\text{ion}} = \sum_I V_{ps}(\mathbf{r} - \mathbf{R}_I)$ is the ionic background potential, V_{ext} the external potential, V_{H} stands for the time-dependent Hartree part and V_{xc} is the exchange-correlation (xc) potential. The electron density is given by $n(\mathbf{r}, t) = \sum_j |\phi_j(\mathbf{r}, t)|^2$. The xc potential $V_{\text{xc}}[n](\mathbf{r}, t)$ is a functional of the time-dependent density and has to be approximated in practice. The simplest choice consists in the TDLDA, defined as

$$V_{\text{xc}}^{\text{TDLDA}}[n](\mathbf{r}, t) = \left. \frac{\delta \epsilon_{\text{xc}}^{\text{hom}}[n]}{\delta n} \right|_{n=n(\mathbf{r}, t)}, \quad (3)$$

where $\epsilon_{\text{xc}}^{\text{hom}}[n]$ is the xc energy density of the homogeneous electron gas. For $\epsilon_{\text{xc}}^{\text{hom}}$ we use the parameterization of Perdew and Wang.⁴⁹ The form of the pseudopotential for a covalent molecule is taken from,⁴⁶ including a non-local part. The TDLDA approximation is augmented by an Average Density Self-Interaction Correction (ADSIC)⁴⁷ to put the single-particle energies at their correct values.

The ground state wave functions are determined by the damped gradient method.⁵⁰ The TDLDA equations are solved numerically by time-splitting technique.⁵¹ The nonlocal part contained in V_{eff} is dealt in an additional propagator and treated with a third-order Taylor expansion of the exponential.⁵² Absorbing boundary conditions are employed to avoid reflecting electrons.⁵³

Ions are treated classically and propagated by classical Molecular Dynamics (MD) equations

$$m_I \frac{d^2 \mathbf{R}_I}{dt^2} = \mathbf{F}_I(\mathbf{R}_I, t) \quad (4)$$

The external perturbation by the laser field, neglecting the magnetic field component, acting both on electrons and ions, is given as

$$V_{\text{ext}, \text{las}} = E_0 z f_{\text{las}}(t) \cos(\omega_{\text{las}} t) \quad (5)$$

where $E_0 \propto \sqrt{I}$, I denoting the intensity, z is the dipole operator, $f_{\text{las}}(t)$ is the pulse profile and ω_{las} is the laser frequency. In this paper, $f_{\text{las}}(t)$ is chosen as a \cos^2 in time.

The external perturbation by a charged projectile is modeled as

$$V_{\text{ext}, \text{ion}} = - \frac{Qe^2}{\sqrt{[x - (v_{\text{proj}} t + x_0)]^2 + y^2 + (z - b)^2}} \quad (6)$$

where Q , v_{proj} , x_0 denote the charge, the velocity and the initial position of the projectile respectively; b is the impact parameter. The excitation amplitude may be tuned through variation of Q , v_{proj} , and b . Here we focus on the influence of Q , b and collision orientation. The velocity is fixed to $v_{\text{proj}} = 20 a_0/\text{fs}$.

The calculations are carried out using a cubic box of size $72 \times 72 \times 64$ with a grid spacing of $0.41 a_0$ and a constant time step $\Delta t = 6 \times 10^{-4}$ fs. The dipole moment can be obtained by $D_i(t) = \int d^3 \mathbf{r} r_i n(\mathbf{r}, t)$, with $i = x, y, z$. The number of escaped electrons is defined as $N_{\text{esc}} = N(t = 0) - \int_V d^3 \mathbf{r} n(\mathbf{r}, t)$, where V is a sufficiently large volume surrounding molecule. A detailed link with experiments is

the probabilities $P^k(t)$ of finding the excited molecule in one of the possible charge states k to which they can ionize. The formula are deduced from the occupied numbers of the time-dependent single-particle orbitals and are taken from.⁵³

3. Results and discussion

3.1. Basic properties of C_2H_4

Fig. 1 shows the spatial structure of ethylene. The molecule is planar and we place

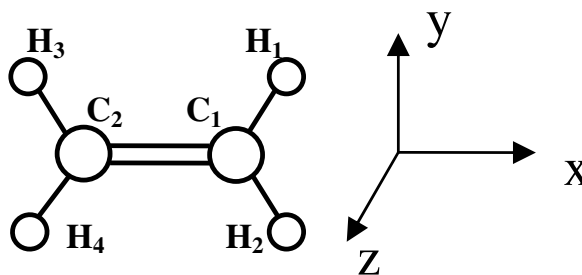


Fig. 1. Ionic structure of ethylene.

it in the x - y plane with two carbon atoms on the x axis and four hydrogen atoms in x - y plane. The center of mass is at the origin. The single-electron energies range from -23.3 eV for the deepest bound valence level to the HOMO at -11.5 eV. The latter is in good agreement with the experimental ionization potential (IP) of 11 eV⁵⁴ (relative error of 4.5 %). Similar errors are obtained when comparing the C-C and the C-H bond lengths (2.43 and 1.97 a_0 respectively, while the experimental values are 2.53 and 2.05 a_0 ⁵⁴).

Fig. 2 shows the optical response, i.e. the photo-absorption strength distribution, of C_2H_4 . It shows strong, isolated peaks at lower energies and changes to a continuum above the IP (11.5 eV). This result is consistent with former TDLDA calculations.⁴⁴ The lowest peak is at 7.74 eV, in good agreement with previous CI calculations (7.76 eV⁵⁵). We obtain the highest peak in the optical response lying at 8.16 eV. The frequency selective laser pulses will be sensitive to this much fluctuating spectrum while a collision with fast ions will deliver a broad spectrum of frequencies and will excite all modes at once.

3.2. Laser excitation

3.2.1. The key role of non-adiabatic couplings

To investigate the effect of the motion of the ionic centers of the molecule on the excitation dynamics, we compare, for the case of a laser excitation, calculations either with full ionic motion or with fixed ionic configuration. The laser intensity is 10^{13} W/cm² and its full width at half maximum (FWHM) is 100 fs. We have

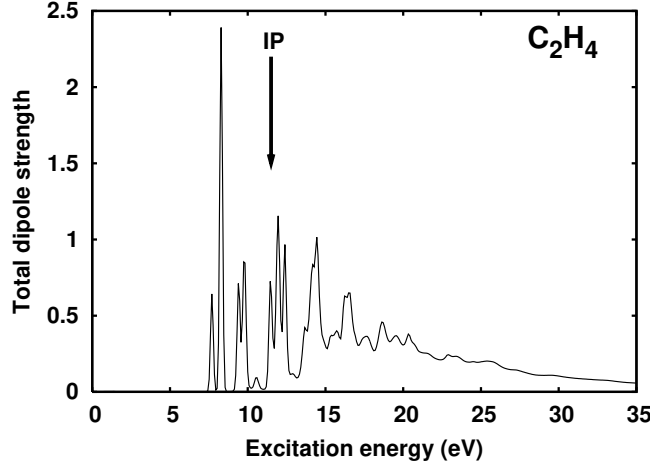


Fig. 2. Total photo-absorption strength of C_2H_4 . The vertical arrow corresponds to the value of the ionization potential of the molecule.

chosen the laser frequency equal to 8.16 eV, that is the value of the highest peak in the optical response (see Fig. 2). We thus expect a resonant excitation of the ethylene. Fig. 3 shows the time evolution of the x ionic coordinates, the number of escaped electrons (N_{esc}), and the dipole moment in the x direction, D_x , for moving and fixed ions. Up to about 35 fs, no significant difference is visible in D_x and N_{esc} . From then on, comparing both cases, the dipole moments diverge rapidly in time and more complex pattern are observed for the case of moving ions. Consequently, the total ionization also differs and more electronic emission is obtained when ions can move (0.8 additional electron is extracted). The ions precisely start to exhibit a sizeable motion at about 40 fs (see top panel). The C-C bond oscillates (see the open squares) while the H (close squares) escape the system, due to the large charge. The non-adiabatic coupling between ions and electrons allows a feed-back of the ionic motion on the electronic response, as can be tracked on the dipole oscillations. The enhancement of ionization for the moving ions case is related to the expansion of the molecule. Indeed, after increasing ionization, the optical spectrum is blue-shifted, so ω_{las} becomes smaller than the resonant frequency. However, the Coulomb force from increased net charge impels the expansion of ions which red-shifts of the optical spectrum and allows ω_{las} to be in the region of resonance again. The difference of electronic emission above shows the importance of treating electronic and ionic dynamics simultaneously.

3.2.2. Scanning laser frequency

To explore in more detail the influence of the laser frequency, we consider two cases, namely $\omega_{\text{laser}} = 9.5$ eV, lying in the resonant region, and $\omega_{\text{laser}} = 6.8$ eV which is off-resonant. Both cases are depicted in Fig. 4 in the left and the right columns respectively. The laser parameters are a polarization along x axis, an intensity of $I = 10^{14}$ W/cm², and a rather short FWHM of 20 fs. The bond lengths and the

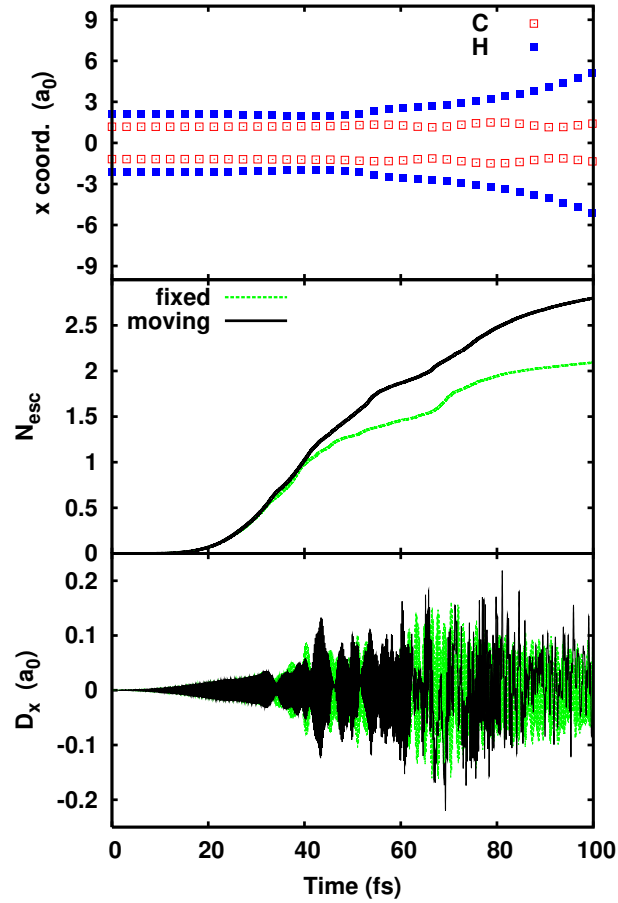


Fig. 3. Excitation of ethylene induced by a laser pulse ($I = 10^{13}$ W/cm², $\omega_{\text{las}} = 8.16$ eV and FWHM of 100 fs), for fixed or moving ions. Top panel: time evolution of the x ionic coordinates, when ionic motion is allowed. Middle and bottom: N_{esc} and dipole moment D_x as a function of time, for moving (dark lines) or fixed (green curves) ions.

r.m.s. radii in the resonant case, top-left panels of Fig. 4, show much different dynamics for the various bonds. The C-H bonds grow quickly and monotonously, which means that the bonds are broken and hydrogen ions are flying apart in the $x-y$ plane. The C-C bond (dark solid line), on the contrary, oscillates with a rather large amplitude during the whole time span. The off-resonant case, top-right panels of Fig. 4, shows regular and faint oscillations for all bonds and r.m.s radii. The molecule remains unfragmented, although highly excited.

The ionization N_{esc} and the dipole evolution shown in the bottom panels of Fig. 4, corroborate these findings. In the off-resonant case (right panels), the dipole nicely follows the laser field, producing an emission of 0.6-0.7 electron during the pulse duration. As soon as the laser is switched off, faint dipole oscillations remain and N_{esc} levels off. The resonant case visibly produces a complex pattern in the dipole evolution with large amplitudes; more ionization is observed, driving the molecule above the limits of binding. Note that N_{esc} starts to increase at around 5

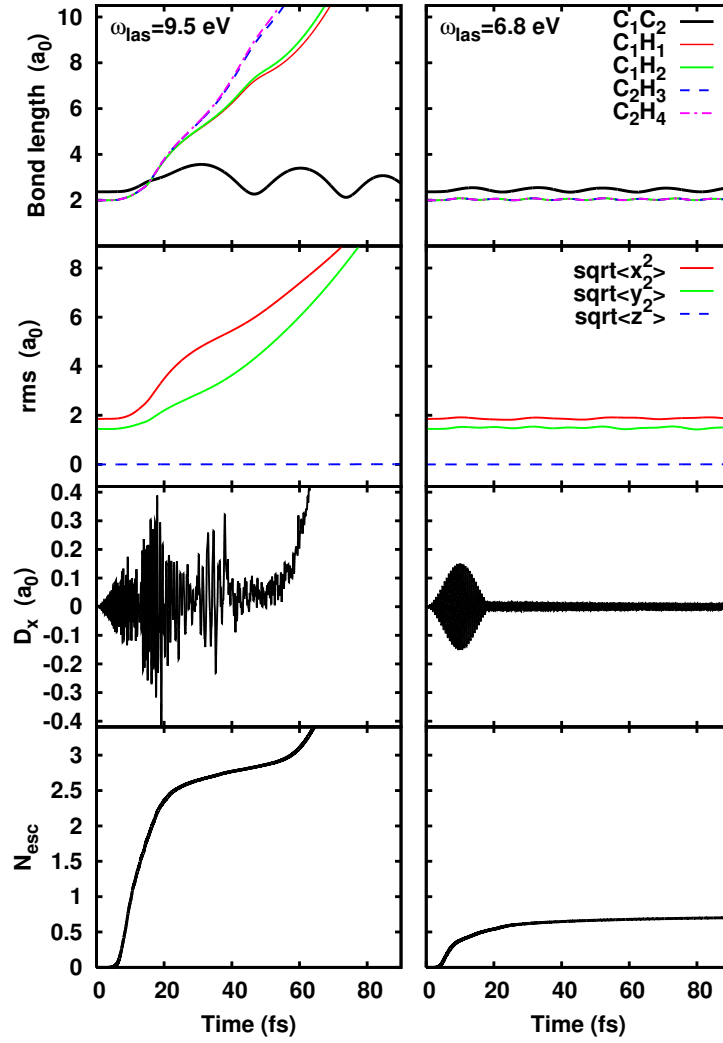


Fig. 4.
Excitation of ethylene
by a laser pulse of
 $I = 10^{14}$ W/cm²,
FWHM of 20 fs,
polarization along
 x axis, for two different
frequencies,
 $\omega_{\text{las}} = 9.5$ eV (left
column), and $\omega_{\text{las}} = 6.8$ eV (right
column). From top
to bottom panels:
time evolution of
bond lengths, ex-
tensions
of
the ionic distribu-
tion in three direc-
tions, dipole signal
along the laser po-
larization and the
number of escaped
electrons.

fs while the ionic motion (see the bond lengths) follows later. Ionization is directly caused by the laser pulse and electrons react quickly because they have a low mass. The ions react indirectly, namely to the Coulomb pressure induced by ionization, and more slowly due to their larger mass.

The above discussion demonstrates the versatility of a laser excitation when playing with its frequency (at low intensities). Indeed the value of this frequency plays an important role in the excitation dynamics of ethylene. In the resonant region, enhanced ionization often leads to a Coulomb fragmentation of the molecule.

3.3. An example of ionic collision

We finally end with a typical example of collision between ethylene and a projectile with charge $Q = 2$. The projectile moves along x direction at the velocity of $20 a_0/\text{fs}$, with an offset of $b = 7 a_0$ in z direction. The initial position of the projectile is $(-100 a_0, 0, 7 a_0)$, thus safely far away from the ethylene. Fig. 5 displays the time evolution of the dipole moments in the three spatial directions, N_{esc} and the ionization probabilities $P^{(n+)}$. Let us start with the dipole response after collision

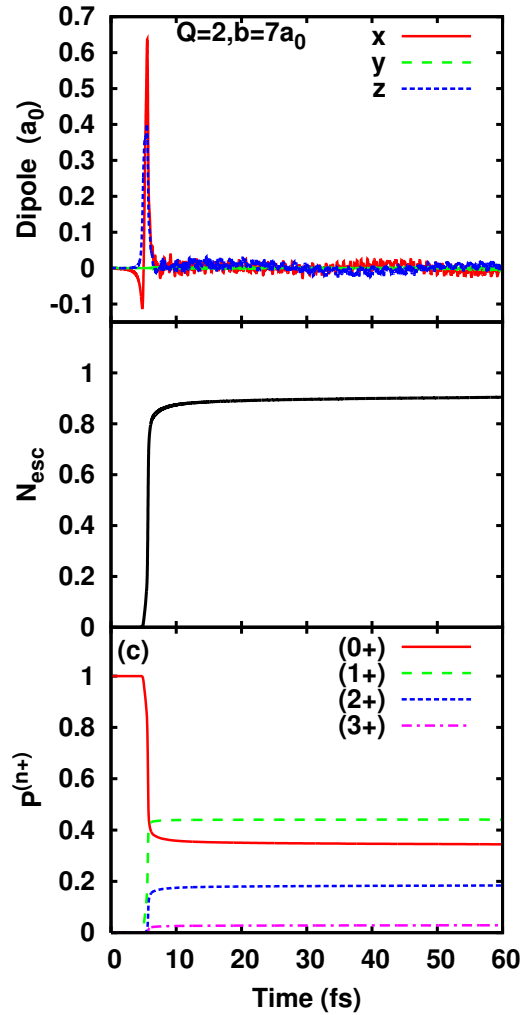


Fig. 5. Time evolution of the dipole moments (top), of the total number of escaped electrons (middle) and ionization probabilities (bottom), after collision of C_2H_4 with a projectile of charge $Q = 2$, impact parameter $b = 7a_0$ and velocity along the x direction of $v_{\text{proj}} = 20 a_0/\text{fs}$.

with the projectile (top panel). Since the projectile moves in the $x - z$ plane along the x axis, no significant excitation along the y direction is expected. And indeed, the dipole moment in that direction, D_y , is vanishingly small. On the contrary, D_x

and D_z exhibit at time of closest approach (at about 5 fs) an almost instantaneous large shift and quickly relax towards much more gentle oscillations that last for a long time. Note that the shift in x direction is higher than that in z direction. This is consistent with the fact that the extension of the electronic cloud is larger in x than in z directions (see the ethylene configuration in Fig. 1). The total ionization, shown in the middle panel of Fig. 5, evolves according to the dipole excitation : it jumps almost immediately at impact time in correlation to the huge dipole moments, while the faint later dipole oscillations do not induce further electron emission. The bottom panel of Fig. 5 shows the detailed ionization probabilities. Their time evolution proceed similarly to that of N_{esc} . Indeed $P^{(0+)}$ falls down abruptly at the time of closest approach, while the other charge state probabilities grow very quickly. Then all probabilities level off and no evolution in time is observed. The charge state 1^+ has the largest probability in accordance with a net ionization of nearly 1 (see middle panel), but a sizeable value of P^{2+} of 20 % is nevertheless attained. As for higher charge states, their probabilities are negligible as expected.

At the side of the ions, this fast collision only induces a visible motion in the $x - y$ plane. More precisely, faint oscillations parallel to the x axis of the C-C bond (aligned with the x axis) are observed, while the C-H bond exhibit larger (but still small) oscillations, because of the smaller mass of the H compared with that of the C. In the y direction, the C atoms simply do not move and the H gently oscillate around their equilibrium positions.

Apart from the different dipole responses, this collision case is close to the off-resonant laser excitation presented in Fig. 4, right column. Indeed, the total ionization there is quite similar (0.7 compared with 0.9 here). However, the ethylene molecule seems able to cope such a ionization and remains in one piece.

Finally, we just mention here some other cases of projectile collision that we have explored. Increasing the charge of the projectile can cause a direct Coulomb fragmentation of the ethylene molecule. We have also varied the value and the direction of the impact parameter b . When the projectile moves perpendicular to the ethylene plane, the electronic response is of course weaker, since the interaction time is shorter than in the case of a projectile moving parallel to the molecular plane. Still the investigated test cases lead us to conclude that the dominant (first order) parameter is the actual (absolute) value of b .

4. Conclusions

In this paper, we have demonstrated the capability of TDLDA-MD to describe complex coupled ionic and electronic excitations. We discussed various excitation scenarios of ethylene subjected to different laser pulses and fast charged projectiles. These scenarios involve both electrons and ions but the relative role of each species does depend on the actual excitation conditions of the laser pulse and charged particles. The response in time of the electron cloud, such as dipole deformation, total number of escaped electrons and ionization probabilities have been presented.

Varying the laser frequency with fixed laser intensity and pulse length indicates that the appearance of de-excitation/explosion scenarios depends on the relationship of the laser frequency with the eigenfrequencies of the system. We have also explored the case of a projectile collision at moderate velocity, a situation that can be easily handled experimentally. A very fast excitation is reported. A systematic study of the dependence on charge, velocity and impact parameter of the projectile will be presented in a forthcoming publication.

ACKNOWLEDGEMENTS

This work was supported by the National Natural Science Foundation of China (Grants No. 10575012 and No. 10435020), the National Basic Research Program of China (Grant No. 2010CB832903), the Doctoral Station Foundation of Ministry of Education of China (Grant No. 200800270017), the scholarship program of China Scholarship Council and the French Agence Nationale pour la Recherche (ANR-06-BLAN-0319-02). Calculations have been performed on the French computational facilities CalMiP, CINES and IDRIS.

References

1. C. von Sonntag, in *The Chemical Basis for Radiation Biology* (Taylor and Francis, London, 1987)
2. B.D. Michael and P.D. O'Neill, *Science* **287**, 1603 (2000)
3. J.de vries, R. Hoekstra, R. Morgenstern, T. Schlathölter, *J. Phys. B* **35**, 4373 (2002)
4. J.de vries, R. Hoekstra, R. Morgenstern, and T. Schlathölter, *Phys. Rev. Lett.* **91**, 053401 (2003).
5. J.de vries, R. Morgenstern, and T. Schlathölter, *Eur. Phys. J. D* **24**, 161 (2003).
6. T. Schlathölter, R. Hoekstra, and R. Morgenstern, *Int. J. Mass Spectrom. Ion Process.* **233**, 173 (2004).
7. T. Schlathölter, R. Hoekstra, S. Zamith, Y. Ni, H.G. Muller, and M. J. J. Vrakking, *Phys. Rev. Lett.* **94**, 233001 (2005).
8. F. Alvarado, R. Hoekstra, and T. Schlathölter, *J. Phys. B* **38**, 4085 (2005).
9. A.M. Sayler, M. Leonard, K.D. Carnes, R. Cabrera-Trujillo, B.D. Esry, and I. Ben-Itzhak, *J. Phys. B* **39**, 1701 (2006).
10. H. Luna and E.C. Montenegro, *Phys. Rev. Lett.* **94**, 043201 (2005).
11. A. Rentenier, P.M. Capelle, D.B. Montesquieu, and A.B. Montesquieu, *J. Phys. B* **38**, 789 (2005).
12. W.S. Melo, A.C.F. Santos, M.M.S. Anna, G.M. Sigaud, and E.C. Montenegro, *J. Phys. B* **39**, 3519 (2006).
13. U. Kreibig, M. Vollmer, *Optical properties of metal clusters* (Springer Series in Materials Science, 1993), Vol. 25.
14. Faisal, *Theory of Multiphoton Processes* (Plenum Press, New York, 1987).
15. J. Zweiback, R. A. Smith, T. E. Cowan, G. Hays, K. B. Wharton, V. P. Yanovsky, and T. Ditmire, *Phys. Rev. Lett.* **84**, 2634 (2000).
16. J. Itatani, J. Levesque, D. Zeidler, H. Niikura, H. Pepin, J. C. Kieffer, P. B. Corkum, and D. M. Villeneuve, *Nature (London)* **432**, 867 (2004).
17. P. B. Corkum and F. Krausz, *Nature Phys.* **3**, 381 (2007).
18. P. Agostini and L. F. DiMauro, *Rep. Prog. Phys.* **67**, 813 (2004).

19. G. Yao and Shih-I Chu, Phys. Rev. A **48**, 485 (1993).
20. K. Sändig, H. Figger, and T. W. Hänsch, Phys. Rev. Lett. **85**, 4876 (2000).
21. T. Zuo and A. D. Bandrauk, Phys. Rev. A **52**, R2511 (1995).
22. T. Seideman, M. Y. Ivanov, and P. B. Corkum, Phys. Rev. Lett. **75**, 2819 (1995).
23. J. P. Hansen, J. Lu, L. B. Madsen, and H. M. Nilsen, Phys. Rev. A **64**, 033418 (2001).
24. J. S. Parker, L. R. Moore, D. Dundas, and K. T. Taylor, J. Phys. B **33**, L691 (2000).
25. S. Chelkowski, T. Zuo, O. Atabek, and A. D. Bandrauk, Phys. Rev. A **52**, 2977 (1995).
26. T. Kreibich, M. Lein, V. Engel, and E. K. U. Gross, Phys. Rev. Lett. **87**, 103901 (2001).
27. A. D. Bandrauk, S. Chelkowski, S. Kawai, and H. Lu, Phys. Rev. Lett. **101**, 153901 (2008).
28. X.-B. Bian, L.-Y. Peng, and T.-Y. Shi, Phys. Rev. A **77**, 063415 (2008).
29. L.-Y. Peng, Q.-H. Gong, and A. F. Starace, Phys. Rev. A **77**, 065403 (2008).
30. A. P. Horsfield, D. R. Bowler, A. J. Fisher, T. N. Todorov, and C. G. Sánchez, J. Phys.: Condens. Matter **17**, 4793 (2005).
31. U. Saalmann and R. Schmidt, Z. Phys. D **38**, 153 (1996).
32. T. Kunert and R. Schmidt, Phys. Rev. Lett. **86**, 5258 (2001).
33. T. Kunert, F. Grossmann, and R. Schmidt, Phys. Rev. A **72**, 023422 (2005).
34. F. Calvo and D. Bonhommeau, and P. Parneix, Phys. Rev. Lett. **99**, 083401 (2007).
35. R. M. Dreizler and E. K. U. Gross, *Density Functional Theory: An Approach to the Quantum Many-Body Problem* (Springer, Berlin, 1990).
36. F. Calvayrac, P.-G. Reinhard, E. Suraud, and C. A. Ullrich, Phys. Rep. **337**, 493 (2000).
37. A. Castro, M. A. L. Marques, J. A. Alonso, G. F. Bertsch, and A. Rubio, Eur. Phys. J. D **28**, 211 (2004).
38. D. Dundas, J. Phys. B **37**, 2883 (2004).
39. E. Suraud and P.-G. Reinhard, Phys. Rev. Lett. **85**, 2296 (2000).
40. F. Calvayrac, P.-G. Reinhard, and E. Suraud, J. Phys. B **31**, 5023 (1998).
41. L. M. Ma, E. Suraud, and P.-G. Reinhard, Eur. Phys. J. D **14**, 217 (2001).
42. M. Ma, P.-G. Reinhard, and E. Suraud, Eur. Phys. J. D **33**, 49 (2005).
43. F. S. Zhang, F. Wang, and Y. Abe, Inter. J. Mod. Phys. B. **19**, 2687 (2005).
44. T. Nakatsukasa and K. Yabana, J. Chem. Phys. **114**, 2550 (2001).
45. M. Ben-Nun and T. J. Martínez, Chem. Phys. **259**, 237 (2000).
46. S. Goedecker, M. Teter, and J. Hutter, Phys. Rev. B **54**, 1703 (1996).
47. C. Legrand, E. Suraud, and P.-G. Reinhard, J. Phys. B **35**, 1115 (2002).
48. E.K.U. Gross and W. Kohn, Adv. Quant. Chem. **21**, 255 (1990).
49. J.P. Perdew and Y. Wang, Phys. Rev. B **45**, 13244 (1992).
50. F. Calvayrac, Ann. Phys. (Paris) **23**, (3) 1 (1998).
51. F. Calvayrac, P.-G. Reinhard, and E. Suraud, Ann. Phys. (NY) **255**, 125 (1997).
52. F. Calvayrac, Ann. Phys. (NY) **255**, 125 (1997).
53. C.A.Ullrich, J. Mol. Struct. (THEOCHEM) **501-502**, 315 (2000).
54. <http://srdata.nist.gov/cccbdb/>.
55. C. Petrongolo, R. J. Buenker, and S. D. Peyerimhoff, J. Chem. Phys. **76**, 3655 (1982).